Extended coupled channels model for πN scattering and the structure of $N^*(1440)$ and $N^*(1535)$

C. Schütz, J. Haidenbauer, and J. Speth
Institut für Kernphysik, Forschungszentrum Jülich GmbH, D-52425 Jülich, Germany

J. W. Durso
Institut für Kernphysik, Forschungszentrum Jülich GmbH, D-52425 Jülich, Germany
and Department of Physics, Mount Holyoke College, South Hadley, Massachusetts 01075
(Received 25 August 1997)

We present a coupled channels model for πN scattering based on N, Δ, and $N^*_{S11}(1535)$ pole and nonpole contributions, plus correlated 2π and a_0 meson exchange. The open channels considered are πN, ηN, σN, and $\pi\Delta$. The model gives a qualitatively good fit to the phase shifts and elasticity parameters in both isospin channels for partial waves up to $J=\frac{3}{2}$ and πN c.m. energies of 1.4 GeV. Above that energy the appearance of resonances in various partial waves precludes a precise fit to the data without explicitly including resonances in those partial waves and—probably—additional inelastic channels. Within the model the $N^*_{S11}(1535)$ resonance appears to require a genuine three-quark component, whereas the $N^*_{P11}(1440)$ resonance appears to permit description as a purely dynamical effect. [S0556-2813(98)01803-2]

PACS number(s): 13.75.Gx, 14.20.Gk, 24.10.Eq, 25.80.Dj

I. INTRODUCTION

Nuclear and intermediate-energy physics may, with some accuracy, be described as the study of effective interactions for hadrons. The objective, ultimately, is to connect the effective interactions with an underlying fundamental theory, i.e., QCD. A more achievable goal, at least for the moment, is the construction of an effective model which unifies related phenomena, such as meson-meson, meson-nucleon, and nucleon-nucleon interactions, in a limited energy domain. It is towards this objective that meson exchange models for $\pi\pi$ and $K\pi$ scattering have been developed [1], and the results of these models incorporated in meson (and baryon) exchange models for KN [2], πN [3,4], and NN [5] scattering. These models are based on effective Lagrangians—that is, on Lagrangians written in terms of the mesonic degrees of freedom—which respect at least some of the symmetries of QCD, such as chiral symmetry, which is especially necessary in $\pi\pi$ and πN systems. Unitarity is found to be extremely important in these systems, so that crossing symmetry is lost in the process of unitarization through a scattering equation. However, the low-energy theorems [6], for example, are obeyed to order m_π^2. This was the motivation behind our previous efforts [3,4], hereafter referred to as I and II, in which we achieved a good quantitative description of S- and P-wave πN phase shifts for pion laboratory momenta up to 500 MeV/c ($\approx$ 300 MeV c.m. kinetic energy). The model included s- and u-channel N and Δ poles, supplemented by $J=0$ and $J=1$ correlated 2π t-channel contributions.

We seek in this work to extend the energy range of I by a factor of approximately 2. Doing this means that we will be investigating an energy domain in which several higher nucleon resonances appear, and in which inelasticity becomes a significant phenomenon. To achieve a reasonably good quantitative fit to the data in this extended energy range requires a significant increase in the complexity of the model through the inclusion of more mesons and more baryon resonances, as well as the adoption of a coupled channels approach for dealing with the inelasticities. The inclusion of higher baryon resonances also means that one must deal with the problem of which resonances are ''genuine,'' i.e., true qqq states which must be included explicitly in the model, and which resonances are generated dynamically by the interactions in the model.

The work we will present is organized as follows. In the next section we will present a discussion of the $\pi N/\eta N$ system and the $N^*_{S11}(1535)$, leading to extensions of our basic model needed for a detailed description of the $S11$ πN partial wave. Section III contains a corresponding discussion of the problems and treatment of the $N^*_{P11}(1440)$, the so-called Roper resonance. In Sec. IV we present the results of the extended model compared with the πN partial wave data for the energy range from 0 to 520 MeV c.m. kinetic energy and conclude in Sec. V with a summary and outlook. The formalism for calculating πN partial wave amplitudes is that of I, to which the reader is referred for details. Formulas specific to the extensions to the basic model of I are given in the Appendix.

II. THE $\pi N/\eta N$ COUPLED CHANNELS AND THE $N^*_{S11}(1535)$ RESONANCE

A. Phenomenology of the $\pi N/\eta N$ system

Since the η meson is, after the pion, the lightest member of the pseudoscalar (Goldstone) boson octet, and contains hidden strangeness, it is a logical candidate for inclusion in our extended model. Furthermore, hadronic reactions in which η mesons are produced are among the most interesting processes in intermediate energy physics. The openings of η production channels lead to clear threshold cusps in

several reactions, such as $\gamma p \to \pi^0 p$, $\gamma p \to \pi^+ n$ [7], or $\pi^- p$ scattering [8]. Even in nuclear reactions, one finds clear signatures of the η threshold [9]. In these, the cross section for η production is, without exception, large. For example, the total reaction cross section for $\pi^- p \to \eta n$ just above the threshold is about 2.7 mb [10], which accounts for about 6% of the total $\pi^- p$ cross section at these energies.

Since the η, in contrast to the π, is an iso*scalar*, η production in $\pi^- p$ scattering acts as an isospin filter, which makes it an especially interesting tool for the investigation of the baryon spectrum. Elastic $\pi^- p$ scattering and the charge-exchange reaction $\pi^- p \to \pi^0 n$ are a mixture of isospin $\frac{1}{2}$ and $\frac{3}{2}$, and are influenced by Δ $(I=\frac{3}{2})$, as well as by N^* $(I=\frac{1}{2})$ resonances. However, the reaction $\pi^- p \to \eta n$ is purely isospin $\frac{1}{2}$, so that only N^* states can be excited in this channel. The production of η's by photons, electrons, as well as hadronic probes is therefore the object of a number of current and planned experiments [9,11–14].

In order to understand all these experiments, an understanding of the η production in the reaction $\pi N \to \eta N$ is of fundamental importance. The theoretical description of this reaction, as well as of the diagonal ηN reaction requires a coupled-channel approach. Since the ηN system can lead to $\pi\pi N$ as well as πN final states, several theoretical models [15–17] therefore employ a third two-body channel to parametrize the other open channels. All the models differ in their various restrictions or approximations, but share the common thread of a direct coupling of π and η to an $N^*_{S11}(1535)$ in order to parametrize the interaction near the η production threshold.

The $N^*_{S11}(1535)$ occupies a very unusual place in the nucleon spectrum as it is the only known resonance that is strongly coupled to the ηN reaction channel. The contribution of the ηN channel to the total decay width of the resonance is, at 30–55 %, about as large as that of the πN channel. The physical nature of the resonance is still a subject of discussion as a result of the work of Höhler [18]. In the speed plot of the $S11$ πN partial wave one finds a sharp maximum at an energy which is indistinguishable from the ηN threshold, but no structure around 1535 MeV. According to Ref. [18], the maximum is the combined contribution of a threshold cusp and a resonance.

These considerations raise the question of whether the $S11$ partial wave's behavior is necessarily due to a genuine three-quark resonance [19–21], or whether it can be understood solely through the dynamics of the opening of the ηN channel. This is the question we will address in the remainder of this section.

B. The coupling of the ηN channel

As the η is a pseudoscalar meson with isospin 0, the contributions to the transition interaction $\pi N \to \eta N$ and to the direct (diagonal) ηN interaction are strongly restricted by selection rules. For example, Δ exchange in the transition interaction is absent because isospin conservation rules out $N\Delta\eta$ vertices. Meson exchange processes for the transition $\pi N \to \eta N$ are limited to isovector mesons with negative G parity, while for the diagonal ηN interaction only exchanges of isoscalar mesons with positive G parity will do. Also,

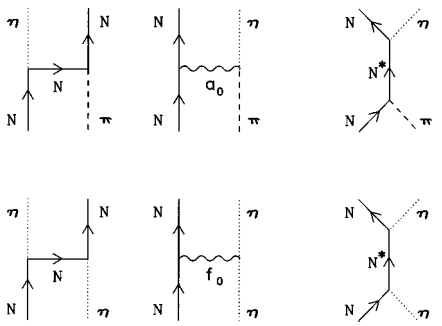

FIG. 1. Additional contributions to the interaction through coupling to the ηN channel.

since three pseudoscalars mesons cannot couple, the lightest mesons to which $\pi\eta$ and $\eta\eta$ can couple are, respectively, the a_0 and the f_0.

The a_0 and f_0 exchange in this work are not to be taken as genuine meson exchanges; rather, they are to be understood as parametrizations of mesonic systems with the corresponding quantum numbers. (This in no way contradicts the interpretation of the a_0 and f_0 as dynamical poles in the meson-meson interaction [22].) Contributions to the interactions from heavier meson exchanges will not be considered explicitly here. The additional contributions to our basic model (I) are illustrated in Fig. 1. The interaction Lagrangians corresponding to the various vertices in the diagrams shown are given by

$$\mathcal{L}_{NN\eta} = \frac{f_{NN\eta}}{m_\pi} \bar{\psi}_N \gamma^5 \gamma^\mu \psi_N \partial_\mu \phi_\eta,$$

$$\mathcal{L}_{NNa_0} = g_{NNa_0}\ \bar{\psi}_N \vec{\tau} \psi_N \cdot \vec{\phi}_{a_0},$$

$$\mathcal{L}_{NNf_0} = g_{NNf_0}\ \bar{\psi}_N \psi_N \phi_{f_0},$$

$$\mathcal{L}_{\pi\eta a_0} = g_{\pi\eta a_0} m_\pi\ \phi_\eta \vec{\phi}_\pi \cdot \vec{\phi}_{a_0},$$

$$\mathcal{L}_{\eta\eta f_0} = g_{\eta\eta f_0} m_\pi\ \phi_\eta \phi_\eta \phi_{f_0},$$

$$\mathcal{L}_{N^*N\pi} = g_{N^*N\pi} \bar{\psi}_{N^*} \vec{\tau} \psi_N \cdot \vec{\phi}_\pi + \text{H.c.},$$

$$\mathcal{L}_{N^*N\eta} = g_{N^*N\eta} \bar{\psi}_{N^*} \psi_N \phi_\eta + \text{H.c.} \tag{2.1}$$

Derivative couplings for the $N^*N\pi$ and $N^*N\eta$ were also considered initially, but were found to give too slow an increase in the phase shift. The expressions for the potentials obtained from these interactions Lagrangians are given in the Appendix.

The potentials for the various contributions contain form factors. For the a_0 and f_0 exchange we use at each vertex a monopole form factor

$$F(\vec{p}_r{}^2) = \frac{\Lambda^2 - m_r^2}{\Lambda^2 + \vec{p}_r{}^2}, \tag{2.2}$$

where the index r denotes the a_0 or the f_0. We adopt the same form for the form factor at the $NN\eta$ vertex in the

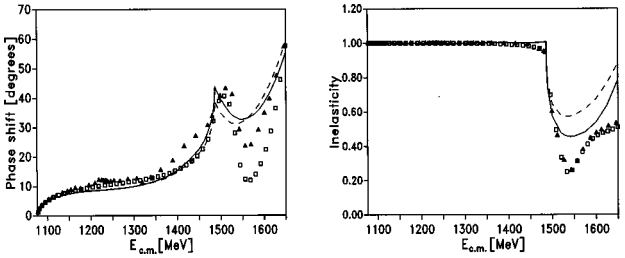

FIG. 2. Attempt at a dynamical explanation of the nucleon resonance $N^*_{S11}(1535)$: phase shift and inelasticity in the S_{11} πN partial wave as a function of the c.m. energy. The solid line shows the results of model B1 and the dashed line those of model B2. The data points are from the Karlsruhe-Helsinki analysis KA84 [27] (solid triangles) and the VPI analysis SM95 [28] (open squares).

nucleon exchange potential, with m_r and $\vec{p}_r$ the mass and momentum of the nucleon. For the N^* pole diagrams we take the form

$$F^{(d)}_{N,\Delta}(\vec{p}^{\,2}) = \frac{\Lambda^{(d)\,4}_{N,\Delta} + m^4_{N,\Delta}}{\Lambda^{(d)\,4}_{N,\Delta} + (E_p + \omega_p)^4} \quad . \tag{2.3}$$

Those coupling constants in Eq. (2.1) not known or fixed by the basic model will be treated as free parameters. With the assumption of $\mathrm{SU(3)_{flavor}} \times \mathrm{SU(2)_{spin}}$ symmetry, we can determine the $NN\eta$ coupling constant if we treat the η as the eighth member of the pseudoscalar octet [23,24] and obtain

$$f_{NN\eta_8} = \frac{0.6}{\sqrt{3}} f_{NN\pi}. \tag{2.4}$$

The $NN\eta$ coupling is thus significantly weaker than the $NN\pi$ coupling.

In the a_0 exchange, the product of the NNa_0 and $\eta\pi a_0$ coupling constants appears. For the NNa_0 coupling we take the value $g^2_{NNa_0}/4\pi = 2.82$ from the full version of the Bonn potential [25]. (Note that the a_0 is denoted as δ in Ref. [25].) As the a_0 mass is greater than the sum of the masses of the π and the η, the a_0 can decay into $\pi\eta$. This is the dominant decay mode of the a_0, so that the $a_0\pi\eta$ coupling can be determined from the a_0 decay width:

$$\Gamma = \frac{g^2_{\pi\eta a_0}}{8\pi} \frac{m^2_\pi}{m^2_{a_0}} p_0, \tag{2.5}$$

where p_0 is the on-shell momentum of the π (or η) in the rest frame of the decaying a_0. Since the width of the a_0 is not well determined, using $m_{a_0} = 983$ MeV and Γ between 50 and 300 MeV, we estimate

TABLE I. Common parameters for models B1, B2, and B3 (see text). Masses and form factor parameters are given in MeV.

m_η	m_{a_0}	m_{f_0}	$\frac{f^2_{NN\eta}}{4\pi}$
547.45	982.7	974.1	0.009336
Λ_{a_0}	Λ_{f_0}	$\Lambda_{NN\eta}$	$\Lambda_{N^*(1535,1650)}$
2500	2500	2500	3000

$$\frac{g_{NNa_0} g_{\pi\eta a_0}}{4\pi} \simeq 6.6 \ldots 16.2. \tag{2.6}$$

As the f_0 is lighter than $2m_\eta$, we cannot make a similar estimate of $g_{\eta\eta f_0}$; therefore, it is treated as a free parameter, as are the bare coupling constants $g^0_{N^*N\pi(\eta)}$ and $f^0_{N^*N\pi(\eta)}$, respectively.

Besides the $N^*_{S11}(1535)$, on which we are concentrating, there is another resonance at higher energy $N^*_{S11}(1650)$. The increase of the $S11$ phase leading to this second resonance is generated by an $N^*_{S11}(1650)$ pole diagram. This contribution is needed as the basis for our investigation of the lower-lying $N^*_{S11}(1535)$. The introduction of this pole diagram parametrizes certain processes which are not explicitly contained in our interaction model, such as the effects of the coupling of the πN system to the strangeness production channels $K\Lambda$ and $K\Sigma$, whose thresholds are at 1611 and 1689 MeV, respectively. Since the direct $K\Sigma$ is very attractive, one can easily imagine that the $N^*_{S11}(1650)$ may have something to do with a quasibound state in this channel [26]. The potentials for the N^* pole contributions are given in Eq. (A6) of the Appendix.

C. Results

As a first step in the analysis of this channel, we wish to learn to what extent the peak in the $S11$ phase shift can be described as a pure threshold phenomenon; that is, as a purely dynamical effect. For this purpose we included only the higher-lying resonance, $N^*_{S11}(1650)$, in the model. The results of two slightly different parametrizations, which we refer to hereafter as models B1 and B2, are shown in Fig. 2, and the corresponding model parameters are given in Tables I and II. (We should point out here that the coupling of the ηN channel has very little effect on the other πN partial waves, with the exception of the $P13$, for which the ηN threshold effect accounts for most of the inelasticity.) Model B1 yields a qualitatively good description of the phase shift and inelasticity (cf. Fig. 2). However, one should be aware that this model is somewhat unrealistic because here also those contributions to the inelasticity which result from other

TABLE II. Parameters for models B1, B2, and B3. The bare N^* masses are given in MeV.

	$\frac{g_{NNa_0} g_{\pi\eta a_0}}{4\pi}$	$\frac{g_{NNf_0} g_{\eta\eta f_0}}{4\pi}$	$\frac{g^{(0)2}_{NN^*_{1535}\pi}}{4\pi}$	$\frac{g^{(0)2}_{NN^*_{1535}\eta}}{4\pi}$	$m^0_{N^*(1535)}$	$\frac{g^2_{NN^*_{1650}\pi}}{4\pi}$	$m^0_{N^*(1650)}$
B1	15	15	0	0	0	0.10	1730
B2	12	15	0	0	0	0.12	1735
B3	8	0	0.001	0.30	1650	0.14	1750

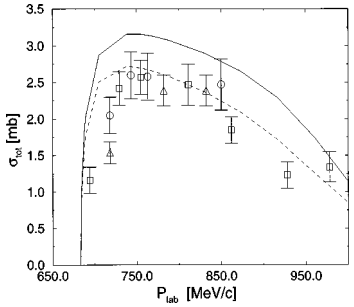

FIG. 3. Total cross section for the reaction $\pi^- p \to \eta n$ as a function of the pion laboratory momentum from the η-production threshold to $E_{\text{c.m.}} \approx 1.65$ GeV. The solid line is the result for model B1 and the dashed line is the result for model B2. The data points are from Refs. [29] (circles), [30] (squares), and [31] (triangles).

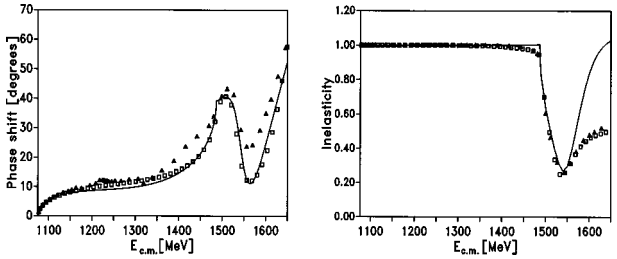

FIG. 4. Phase shift and inelasticity in the S_{11} πN partial wave in model B3, which includes the contribution of a genuine $N^*_{S11}(1535)$ resonance. The data points are from the Karlsruhe-Helsinki analysis KA84 [27] (solid triangles) and the VPI analysis SM95 [28] (open squares).

open channels, especially $\pi\pi N$, are parametrized into the ηN channel. One recognizes this when one calculates the total cross section for η production in the reaction $\pi^- p \to \eta n$. As Fig. 3 shows, the prediction of model B1 is about 15% too large. If we reduce the strength of the $\pi N \to \eta N$ transition interaction by reducing the a_0 exchange coupling (model B2; cf. Table II), the $\pi^- p \to \eta n$ cross section can be described fairly well; only the threshold region is overestimated. However, it can be seen from Fig. 2 that the inelasticity produced by model B2 is now distinctly smaller than for model B1. Clearly, other reaction channels, besides ηN, are needed in order to reproduce the inelasticity of the $S11$ πN partial wave and the η-production cross section consistently.

Although the description of the $S11$ partial wave amplitude in this model—which contains no explicit $N^*_{S11}(1535)$—is qualitatively good, the models display significant deviation from the data. In these two variations of the model, the maximum in the phase shift is a threshold cusp due to the opening of the ηN channel, and sits exactly on the threshold, $E_{\text{c.m.}} \approx 1487$ MeV. In both the Karlsruhe-Helsinki partial wave analysis [27], and the more recent VPI analysis [28], the maximum in the phase shift lies at a distinctly higher energy, namely, at approximately 1515 MeV. (Evidently, the maximum of the $S11$ phase shift lies at a somewhat higher energy than the maximum found in the speed plot of this partial wave, discussed earlier in this paper.) No reasonable variation of the coupling constants can shift the position of the maximum; it is fixed by the ηN threshold. Insofar as the partial wave analyses are reliable, the description of the $N^*_{S11}(1535)$ as a threshold phenomenon must be considered incomplete.

The description of the $S11$ partial wave can be significantly improved by the inclusion of a ''true'' $N^*_{S11}(1535)$ pole contribution with a relatively strong coupling to the ηN channel, which we call model B3 (see Table II). This strong coupling to the $N^*_{S11}(1535)$ resonance, compared with the very weak coupling to the $N^*_{S11}(1650)$ (which we hereafter neglect), can be explained in quark models of baryons [19,20] by a strong mixing of three-quark states with total spin $\frac{1}{2}$ and $\frac{3}{2}$.

As shown in Fig. 4, the $S11$ phase and inelasticity in the region of the $N^*_{S11}(1535)$ is now even quantitatively well described—after the above addition to our model. This is essentially the result of a direct $N^* N \eta$ coupling; the contribution of f_0 exchange to the diagonal ηN interaction is negligible. As we discussed previously, this leads to a prediction for the η production cross section which is somewhat too large. One could include coupling to other purely phenomenological channels [15–17], as in earlier studies, but this would be just a parametrization of the scattering data and will not be pursued here. As explained above, a full microscopic description of the $S11$ partial wave in this energy range also calls for an understanding of the strangeness production channels $K\Lambda$ and $K\Sigma$, in addition to explicit consideration of pion production [26]. Nevertheless, as the results of our present model B3 are in much better agreement with the phase shift analysis than models B1 and B2, it appears very probable that there is a genuine three-quark component of the $N^*_{S11}(1535)$.

III. THE NATURE OF THE ROPER RESONANCE

A. Phenomenology of the Roper resonance

In the spectrum of the nucleon and Δ resonances, the Roper resonance $N^*_{P11}(1440)$ occupies a special place. It is at once noteworthy that this resonance produces no immediately observable signature in the observables of πN scattering. Whereas, for example, the resonance $N^*_{D13}(1520)$ can be identified with a maximum in the total $\pi^- p$ cross section, the Roper resonance produces no separate extremum at lower energies; rather it contributes only to the background of the other resonances. It is necessary to carry out a partial wave analysis in order to recognize the Roper resonance. It was only relatively recently that it was directly confirmed in a hadronic reaction [32].

Indeed, the attempt to understand the Roper resonance theoretically in the framework of the quark model leads to considerable difficulties [19,20]. The Roper resonance is the first excited N^* state of the nucleon, and it has *positive* parity. In the spectrum of observed nucleon resonances, the Roper is followed in energy by two groups of resonances with *negative* parity $N^*_{S11}(1535)$ and $N^*_{D13}(1520)$, as well as by a triplet $N^*_{S11}(1650)$, $N^*_{D13}(1700)$, and $N^*_{D15}(1675)$, also of negative parity, at slightly higher energy.

These N^* states of negative parity can be immediately understood in a simple quark model [19]. There one employs the ansatz of a flavor-independent harmonic oscillator potential to provide confinement, and the residual interaction of the quarks is modeled by a term of the form $\vec{\sigma}_i \cdot \vec{\sigma}_j$, which is

motivated by the one-gluon exchange. Excitation of quarks from the ground state to a state with orbital angular momentum $L=1$ (excitation of the oscillator by $1\,\hbar\omega$) results in the pair of N^* resonances through the coupling of the total spin of the quarks $S=\frac{1}{2}$ with $L=1$ to $J=\frac{1}{2}$ and $J=\frac{3}{2}$. The triplet at higher energy corresponds to quark spin $\frac{3}{2}$ coupled with $L=1$ to $J=\frac{1}{2}$, $J=\frac{3}{2}$, and $J=\frac{5}{2}$. In this admittedly oversimplified picture, one immediately obtains an obvious explanation of the nucleon resonances with negative parity.

How can an excited state of the nucleon with positive parity, based on the harmonic oscillator, be understood? The energetics of the lowest-lying excited state with positive parity is the result of the excitation of quarks to $2\,\hbar\omega$ with $L=0$ and $L=2$. Such an excited state should lie higher in energy than the $L=1$ excited states, which we have identified with the negative-parity nucleon resonances. The explanation of the Roper resonance as a radial excitation of the nucleon in the quark model requires large additional interaction terms to bring the energy of this excited state to a value below the energies of the negative-parity resonances. In comparison with the N^*s with negative parity, the explanation of the Roper resonance appears less intuitive.

Several models of the Roper resonance have been developed. For example, the model of Brown *et al.* [33] produces the resonance through the anharmonic collective oscillation of a bag surface. In this model, however, one obtains no satisfactory description of the πN scattering data, as the width of the resonance is too small. Isgur and Karl [19,20] attribute the lowering of the positive-parity state to a large, first-order, anharmonicity in the confining potential, whereas Glozman and Riska [21] produce it through flavor symmetry breaking in the exchange of the pseudoscalar mesons in the residual quark-quark interaction due to the large mass differences in the pseudoscalar octet. Finally, on a somewhat different footing, Pearce and Afnan studied the Roper resonance in a Faddeev-type three-body calculation employing interactions based on the cloudy bag model [34]. However, regardless of the scheme, a quantitative description of the scattering data is lacking.

In parallel with the preceding section, we wish to ask again the question of to what extent the Roper resonance can be understood as a product of the dynamics of our meson exchange model. We have already seen in I that the rise of the $P11$ phase leading to the Roper resonance in the region of elastic scattering, can be reproduced without a genuine three-quark resonance. In an extension of the energy domain of our model above the energy of the Roper resonance, we should observe that the $P11$ partial wave is *the* partial wave of the πN interaction which shows significant inelasticity at the lowest energy (≈ 1.3 GeV). Therefore the investigation of the Roper resonance requires the consideration of pion production processes. These take place in our model through the coupling to the reaction channels $\pi\Delta$ and σN. Thus, the $\pi\Delta$ channel describes a $\pi\pi N$ intermediate state in which a pion and the nucleon form a $P33$ state, and the σN intermediate state represents a correlated $\pi\pi$ subsystem in the scalar-isoscalar channel of the $\pi\pi$ interaction.

B. The coupling of the reaction channels $\pi\Delta$ and πN

We start with the coupling of the $\pi\Delta$ channel shown in the diagrams in Fig. 5. Both in the transition interaction $\pi N\rightarrow\pi\Delta$ and in the diagonal $\pi\Delta$ interaction we take into account nucleon, Δ, and ρ exchange processes.

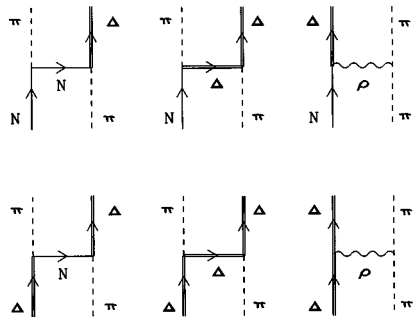

FIG. 5. Diagrams considered in the transition interaction $\pi N\rightarrow\pi\Delta$ and in the diagonal $\pi\Delta$ interaction.

In addition, one could consider the exchange of a σ meson in the diagonal $\pi\Delta$ interaction. We do not take this contribution explicitly into account for a number of reasons. All of the diagrams introduced in the diagonal $\pi\Delta$ interaction of our model give attractive potentials in the $P11$ partial wave. This attraction in the $\pi\Delta$ channel will be dominated by ρ meson exchange. The coupling constants $f_{\Delta\Delta\pi}$, $f_{N\Delta\rho}$, and $g^{(V,T)}_{\Delta\Delta\rho}$ given by the SU(2)×SU(2) quark model [35] (see also Ref. [25]) are to be interpreted only as estimates. The additional effect of a σ-exchange potential can easily be accommodated by a slight variation of the parameters for the vertices considered here.

In a complete microscopic model one should treat the σ and ρ exchanges in the diagonal $\pi\Delta$ channel as correlated 2π exchange processes, analogously to our procedures in II for the πN channel. The starting point for this would be a dynamical model for the $\Delta\bar{\Delta}\rightarrow\pi\pi$ reaction. In contrast with our model for the 2π exchange in the πN channel, one cannot fix parameters by comparison with quasiempirical amplitudes; one can at best arrive at only an estimate of the correlated 2π exchange in the $\pi\Delta$ interaction. We choose, therefore, a more phenomenological treatment for the diagonal $\pi\Delta$ interaction.

The contributions of the various processes in Fig. 5 are evaluated using the interaction Lagrangians

$$\mathcal{L}_{\Delta\Delta\pi}=-\frac{f_{\Delta\Delta\pi}}{m_\pi}\bar{\psi}_{\Delta\,\nu}\,\gamma^5\gamma^\mu\,\vec{T}\,\psi^\nu_\Delta\cdot\partial_\mu\vec{\phi}_\pi,$$

$$\mathcal{L}_{\Delta\Delta\rho}=-\bar{\psi}_{\Delta\,\zeta}\left\{g^V_{\Delta\Delta\rho}\gamma_\mu\vec{\phi}_\rho^{\,\mu}+\frac{1}{4m_\Delta}g^T_{\Delta\Delta\rho}\sigma_{\mu\nu}(\partial^\mu\vec{\phi}_\rho^{\,\nu}-\partial^\nu\vec{\phi}_\rho^{\,\mu})\right\}\cdot\vec{T}\psi^\zeta_\Delta,$$

$$\mathcal{L}_{N\Delta\rho}=i\frac{f_{N\Delta\rho}}{m_\rho}(\bar{\psi}_N\gamma^5\gamma^\mu\vec{T}\psi^\nu_\Delta-\bar{\psi}^\nu_\Delta\gamma^5\gamma^\mu\vec{T}^\dagger\psi_N)\cdot(\partial_\mu\vec{\rho}_\nu-\partial_\nu\vec{\rho}_\mu),\tag{3.1}$$

in addition to $\mathcal{L}_{NN\pi}$, $\mathcal{L}_{N\Delta\pi}$, and $\mathcal{L}_{\rho\pi\pi}$ given in I. Expressions for the potentials corresponding to the Lagrangians in Eq. (3.1) appear in the Appendix.

With the addition of the coupling to the σN reaction channel, we consider the processes shown in Fig. 6. Our

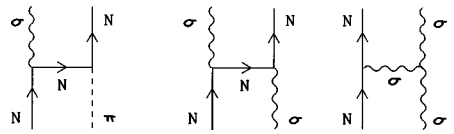

FIG. 6. Contributions to the interaction model from coupling to the σN channel.

model for the $\pi N \to \sigma N$ transition interaction therefore does not contain the diagram for the pion exchange from Fig. 7(a), which would also appear to contribute. Were we to introduce this into our model, iteration of the scattering equation would result in the contribution to the πN interaction shown in Fig. 7(b). This contribution, however, is implicitly contained in our model for the correlated 2π exchange in the πN interaction. Inclusion of the single pion exchange would then lead to double counting. (At this point we must also point out that the inclusion of these diagrams in our model, which is based on time-ordered perturbation theory, would cause significant technical difficulties. For energies above the $\pi\pi N$ threshold the $\pi\pi N$ intermediate state gives rise to a cut [see Fig. 7(c)]. Without the consistent accounting for all contributions of the same order to the interaction, especially that of the nucleon self-energy, the cut would result in a violation of unitarity.)

The potentials corresponding to the diagrams of Fig. 6 follow from the interaction Lagrangians

$$\mathcal{L}_{NN\sigma} = g_{NN\sigma} \bar{\Psi}_N \Psi_N \phi_\sigma ,$$

$$\mathcal{L}_{\sigma\sigma\sigma} = g_{\sigma\sigma\sigma} m_\sigma \phi_\sigma \phi_\sigma \phi_\sigma , \tag{3.2}$$

and are given in the Appendix. For the effective $NN\sigma$ coupling we use the value from Ref. [36]; the coupling constant $g_{\sigma\sigma\sigma}$ we take as a free parameter and adjust it to the scattering data. For the (renormalized) σ mass we take the value from the energy at which the δ_{00} $\pi\pi$ phase shift passes through 90°, thus $m_\sigma = 850$ MeV.

The vertices in the diagrams of Figs. 5 and 6 have form factors. The $NN\pi$ form factor is fixed by the nucleon exchange in the πN channel. For the other vertices we use form factors of the form given in Eq. (2.2). At the vertices where a Δ appears, the square of the form is used in order to ensure convergence.

C. The self-energies of the Δ isobar and σ meson

With the Δ isobar in the $\pi\Delta$ channel and the σ meson in the σN channel we are not dealing with stable particles. Rather, the Δ and σ here stand for πN and $\pi\pi$ subsystems with the quantum numbers of the $P33$ partial wave in the πN system and the $I = J = 0$ partial wave in the $\pi\pi$ system, respectively. In order to simulate these, we adopt a simplified

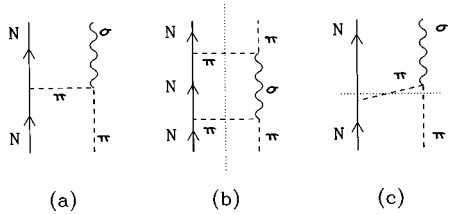

FIG. 7. Pion exchange in the transition interaction $\pi N \to \sigma N$.

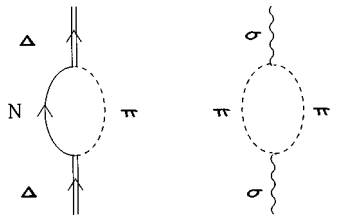

FIG. 8. Self-energy contributions of the Δ isobar and the σ meson.

model for both the $P33$ πN partial wave and the δ_{00} $\pi\pi$ partial wave in which pole diagrams, in the framework of time-ordered perturbation theory, are iterated (see Fig. 8). Hereafter we take expressions for the self-energies of the Δ and σ which appear in the propagators of the $\pi\Delta$ and σN intermediate states in our scattering equation

$$G_{\pi\Delta}(Z,p) = \frac{1}{Z - \sqrt{m_\pi^2 + p^2} - \sqrt{(m_\Delta^0)^2 + p^2} - \Sigma_\Delta(Z,p)} ,$$

$$G_{\sigma N}(Z,p) = \frac{1}{Z - \sqrt{m_N^2 + p^2} - \sqrt{(m_\sigma^0)^2 + p^2} - \Sigma_\sigma(Z,p)} . \tag{3.3}$$

By taking into account the self-energy contributions we preserve the correct threshold behavior for the description of pion production in the πN system.

One should recall that in I and II we introduced realistic models for $\pi\pi$ scattering in the $I = J = 0$ partial wave and for πN scattering in the $P33$ partial wave. In this section, for technical reasons, the models for Δ isobar and for the σ meson stand, in contrast, as effective parametrizations of the $\pi\pi$ and πN T matrices in the corresponding partial waves.

The $P33$ πN partial wave in the region of the Δ resonance can be well approximated by a direct pole contribution as given by Eq. (A3) of I if the bare parameters of the Δ are suitably adjusted. In Fig. 9 we show the model with the parameters $m_\Delta^0 = 1415$ MeV, $f_{N\Delta\pi}^{(0)2}/4\pi = 0.36$, and $\Lambda_\Delta^{(d)} = 1500$ MeV, which we use to calculate the self-energy of the Δ in this work. Following I, the iteration of a pole diagram of the form

$$V^P = \frac{v_0 v_0^\dagger}{Z - m^0} \tag{3.4}$$

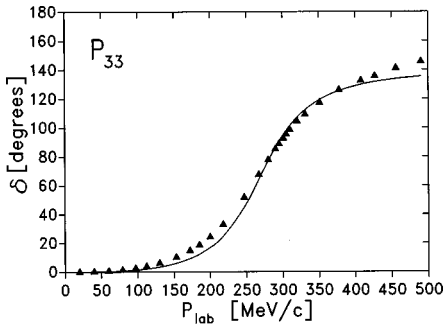

FIG. 9. Approximation of the P_{33} partial wave in πN scattering by a Δ pole diagram: πN phase shift as a function of the pion laboratory momentum. The data are from Ref. [37].

results in the T matrix

$$T=\frac{v_0 v_0^\dagger}{Z-m^0-\Sigma}, \tag{3.5}$$

where v^0 stands for the vertex (here, $\Delta\to\pi N$) and Σ for the self-energy which, in the rest frame of the Δ, is given by

$$\Sigma_\Delta(Z_\Delta)=\int q^2 dq\,\frac{v_0^{N\Delta\pi}(q)[v_0^{N\Delta\pi}(q)]^\dagger}{Z_\Delta-E_N(q)-\omega_\pi(q)}. \tag{3.6}$$

The self-energy of the Δ is a function of the energy Z_Δ of the isobar. For a moving Δ intermediate state one carries this energy through, so that one subtracts the energy of the spectator pion and the kinetic energy of the Δ isobar from the total energy of the $\pi\Delta$ system:

$$\begin{aligned}Z_\Delta(Z,p)&=Z-\omega_\pi(p)-E_\Delta^{\rm kin}(p)\\&=Z-\omega_\pi(p)-[\sqrt{(m_\Delta^0)^2+p^2}-m_\Delta^0].\end{aligned} \tag{3.7}$$

For the description of $\pi\pi$ scattering in the δ_{00} partial wave, we start from a σ pole diagram. We calculate the corresponding expression for the potential from the interaction Lagrangian

$$\mathcal{L}_{\pi\pi\sigma}=g_{\pi\pi\sigma}m_\pi\vec{\phi}_\pi\cdot\vec{\phi}_\pi\,\phi_\sigma, \tag{3.8}$$

from which one finds, after a partial wave decomposition,

$$\begin{aligned}\langle q'|V_\sigma^{\rm Pol}|q\rangle=48\pi\, g_{\pi\pi\sigma}^2 m_\pi^2&\frac{1}{(2\pi)^3\,2\omega_\pi(q)2\omega_\pi(q')}\\&\times\frac{1}{2m_\sigma^0}\frac{1}{Z-m_\sigma^0}F(q)F(q'),\end{aligned} \tag{3.9}$$

where q, q' are the moduli of the relative $\pi\pi$ three-momentum in the c.m. system (i.e., $q=|\vec{q}|$). For the form factors we use the monopole ansatz $F(q)=\Lambda_{\pi\pi\sigma}^2/(\Lambda_{\pi\pi\sigma}^2+q^2)$. By comparison with Eq. (3.4), one obtains for the $\pi\pi\sigma$ vertex

$$v_0^{\pi\pi\sigma}(q)=\frac{\sqrt{3}\,g_{\pi\pi\sigma}m_\pi F(q)}{\pi\,2\omega_\pi(q)\sqrt{\omega_\sigma^0}}. \tag{3.10}$$

In the denominator of Eq. (3.9) the factor m_σ^0 stands for the on-mass-shell energy ω_σ^0 of the bare σ meson which, in the rest frame, is given by the bare mass. For the calculation of the σ self-energy in a moving frame, one must use the on-mass-shell energy ω_σ^0, as in Eq. (3.10). One gets the T matrix for our effective model of $\pi\pi$ scattering in this partial wave from Eq. (3.5), in which the self-energy here is given by

$$\Sigma_\sigma(Z_\sigma)=\int q^2 dq\,\frac{v_0^{\pi\pi\sigma}(q)[v_0^{\pi\pi\sigma}(q)]^\dagger}{Z_\sigma-2\omega_\pi(q)}. \tag{3.11}$$

As one can see from Fig. 10, the δ_{00} $\pi\pi$ partial can be reasonably well described with our simple, effective model. The parameters used here are m_σ^0 = 900 MeV, $g_{\pi\pi\sigma}$ = 9.5, and $\Lambda_{\pi\pi\sigma}$ = 1500 MeV.

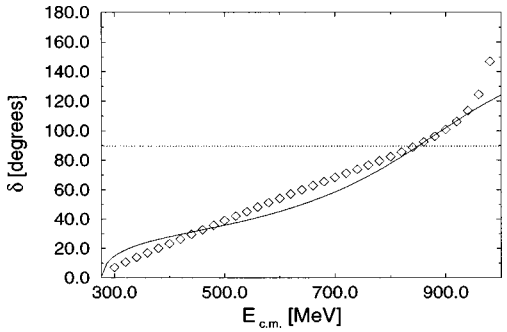

FIG. 10. Approximation of the δ_{00} partial wave in $\pi\pi$ scattering by a σ pole diagram: $\pi\pi$ phase shift as a function of the c.m. energy of the $\pi\pi$ system. The data are from [38].

In the propagation of a σN intermediate state according to Eq. (3.3) the $\pi\pi$ system is not at rest. The energy Z_σ available to the $\pi\pi$ subsystem is obtain by subtracting the energy of the spectator nucleon and the kinetic energy of the σ from the total energy Z of the σN system:

$$\begin{aligned}Z_\sigma(Z,p)&=Z-E_N(p)-E_\sigma^{\rm kin}(p)\\&=Z-E_N(p)-[\sqrt{(m_\sigma^0)^2+p^2}-m_\sigma^0].\end{aligned} \tag{3.12}$$

D. A dynamical model for the Roper resonance

In the preceding sections we have laid the groundwork for the development of a coupled-channels treatment of the πN system from threshold to the energy domain of significant inelasticity. As a penultimate step in this development we present in this section a dynamical model for the Roper resonance. It should be noted here that we aim at a description of the $P11$ partial wave with a parameter set that yields also a consistent picture for all other πN partial waves as well. A discussion of our full coupled-channel model for energies up to $E_{\rm c.m.}$=1.6 GeV will be given in the next section.

We develop the model for the Roper resonance in stages. The starting point is a variation on model 2 of II, for which the ingredients are the direct (pole) and exchange contributions of nucleons and Δ isobars, as well as correlated 2π exchange in the σ and ρ channels. The first stage, using these contributions, is to open the $\pi\Delta$ channel, and readjust some parameters. This simple, two-coupled-channels model (called model C in the following) allows for some inelasticity, which is missing from the earlier model. The processes considered are shown in Fig. 5. It makes sense to introduce the $\pi\Delta$ channel first, since it couples with all the partial waves we are treating in this work, in particular also to those with $I=\frac{3}{2}$. By contrast, the influence of the σN channel is limited to partial waves with $I=\frac{1}{2}$, and, practically speaking, is of relevance only for the $P11$ partial wave.

The results for this model (dash-dotted curve) are compared with those of the purely elastic scattering model (dashed curve) in Fig. 11, and the relevant parameter sets are given in Tables III and IV. One can see that the basic model gives a very good description of the phase shift up to $E_{\rm c.m.}$ $\approx$1.45 GeV. However, since the model has only one channel, the inelasticity is necessarily 1. As can be seen in the lower part of the figure, in both the Karlsruhe-Helsinki [27]

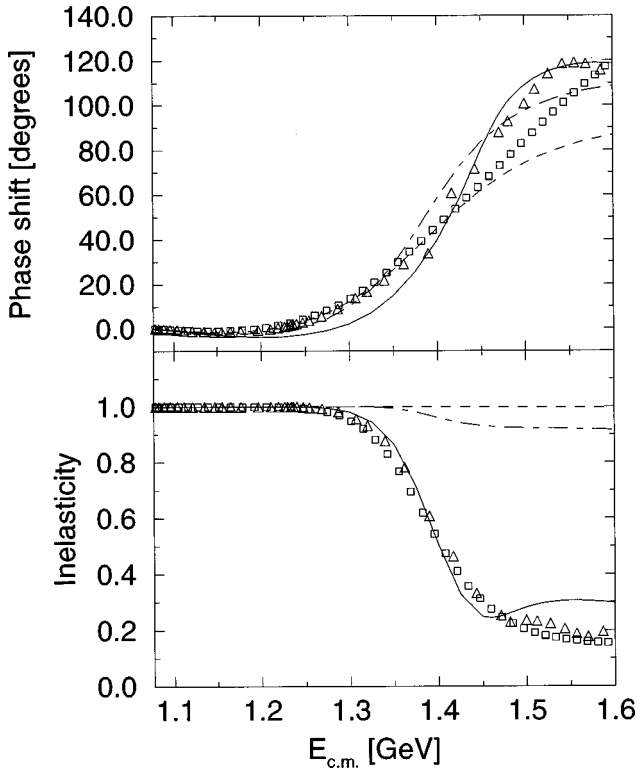

FIG. 11. A dynamical model for the Roper resonance: phase shift and inelasticity in the $P11$ partial wave in πN scattering as a function of the c.m. energy. The dashed line indicates the extrapolation of the basic πN model (see Table III), the dash-dotted line is the coupled-channel model $\pi N/\pi\Delta$ (model C), and the solid line the full coupled-channel model $\pi N/\eta N/\pi\Delta/\sigma N$ (model D). The data are from the Karlsruhe-Helsinki analysis KA84 [27] (triangles) and the VPI analysis SM95 [28] (squares).

and the VPI [28] partial wave analyses, significant inelasticity sets in at about 1.3 GeV.

In I it was explained that the bare parameters $f^0_{NN\pi}$ and m^0_N of the nucleon pole diagram in our model for elastic πN scattering were determined by a renormalization procedure [39] in such a way that the resulting T matrix had a pole at the physical nucleon mass, whose residue determines the physical πNN coupling. In the coupled-channel model we have developed here, we take into account the influence of all the reaction channels on the renormalization of the nucleon pole diagram. The exact renormalization of the nucleon is thus guaranteed in our calculation.

TABLE III. The parameters for the basic (uncoupled) model. Masses and form-factor parameters Λ are given in MeV.

m_π	m_N	m_Δ	m^0_N	m^0_Δ	
138.03	938.926	1232	1053.791	1370	
$\frac{f^2_{NN\pi}}{4\pi}$	$\frac{f^{(0)2}_{NN\pi}}{4\pi}$	$\frac{f^2_{N\Delta\pi}}{4\pi}$	$\frac{f^{(0)2}_{N\Delta\pi}}{4\pi}$		
0.0778	0.0476	0.36	0.21		
$\Lambda^{(d)}_N$	$\Lambda^{(\mathrm{ex})}_N$	$\Lambda^{(d)}_\Delta$	$\Lambda^{(\mathrm{ex})}_\Delta$	Λ_σ	Λ_ρ
1270	1300	1500	2000	1150	1600

TABLE IV. Coupling constants, bare masses, and form-factor parameters Λ for the coupled-channel calculation $\pi N/\pi\Delta$ (model C). All masses and form-factor parameters are given in MeV.

Vertex	Process	Coupling constant	Λ
correlated 2π	ρ channel		1500
exchange	σ channel		1150
$NN\pi$	N exchange	$\frac{f^2_{NN\pi}}{4\pi}=0.0778$	1300
$NN\pi$	N pole, $m^0_N=1093.289$	$\frac{f^{(0)2}_{NN\pi}}{4\pi}=0.0439$	1380
$N\Delta\pi$	$N-$, Δ exchange	$\frac{f^2_{N\Delta\pi}}{4\pi}=0.36$	2000
$N\Delta\pi$	Δ pole, $m^0_\Delta=1420$	$\frac{f^{(0)2}_{N\Delta\pi}}{4\pi}=0.21$	1700
$\Delta\Delta\pi$	Δ exchange	$\frac{f^2_{\Delta\Delta\pi}}{4\pi}=0.252$	1800
$N\Delta\rho$	ρ exchange	$\frac{f^2_{N\Delta\rho}}{4\pi}=20.45$	1500
$\Delta\Delta\rho$	ρ exchange	$\frac{g^{V2}_{\Delta\Delta\rho}}{4\pi}=4.69$	1500
		$\frac{g^T_{\Delta\Delta\rho}}{g^V_{\Delta\Delta\rho}}=6.1$	
$\pi\pi\rho$	ρ exchange	$\frac{g^2_{\pi\pi\rho}}{4\pi}=2.90$	1500

As can be seen in the upper part of Fig. 11, the coupling of the $\pi\Delta$ channel (model C) already gives rise to a resonant behavior in the $P11$ partial wave at the correct energy. On the other hand, as is evident in the lower part of the figure, the influence of the $\pi\Delta$ channel has only a slight effect on the inelasticity. The fit to the $P11$ data can be improved—by raising the form factor mass for the $\pi N\rightarrow\pi\Delta$ transition, for example—but only at the cost of a much worse description of the other πN partial waves. This particular example would result in an inelasticity in the $P33$ partial wave which is too large.

At this stage one should note that the accounting for the different contributions to the transition interaction $\pi N\rightarrow\pi\Delta$ is of great importance to the understanding of the scattering data. While in the $P11$ partial wave the ρ, N, and Δ exchanges have all the same sign (attractive), the nucleon exchange changes sign in the isospin $\frac{3}{2}$ channel. As a result, the different contributions in the $P31$ wave partially cancel one another, and we get a very small net contribution to the inelasticity, which is in agreement with the data. Taking only ρ exchange in the $\pi N\rightarrow\pi\Delta$ transition would result in a large inelasticity in the $P31$ wave, because of the larger isospin factor for $I=\frac{3}{2}$, but hardly any inelasticity in the $P11$, in strong contrast to the data.

The description of the $P11$ partial wave can be significantly improved by the additional coupling of the σN reac-

TABLE V. Coupling constants, bare masses and form-factor parameters Λ for the coupled-channel calculation $\pi N/\pi\Delta/\sigma N/\eta N$ (model D). All masses and form-factor parameters are given in MeV.

Vertex	Process	Coupling constant	Λ
correlated 2π	ρ channel		1400
exchange	σ channel		1150
$NN\pi$	N exchange	$\frac{f^2_{NN\pi}}{4\pi}=0.0778$	1300
$NN\pi$	N pole, $m^0_N=1110.456$	$\frac{f^{(0)\,2}_{NN\pi}}{4\pi}=0.0508$	1410
$N\Delta\pi$	N, Δ exchange	$\frac{f^2_{N\Delta\pi}}{4\pi}=0.36$	1800
$N\Delta\pi$	Δ pole, $m^0_\Delta=1405$	$\frac{f^{(0)\,2}_{N\Delta\pi}}{4\pi}=0.21$	1650
$\Delta\Delta\pi$	Δ exchange	$\frac{f^2_{\Delta\Delta\pi}}{4\pi}=0.252$	1800
$N\Delta\rho$	ρ exchange	$\frac{f^2_{N\Delta\rho}}{4\pi}=20.45$	1400
$\Delta\Delta\rho$	ρ exchange	$\frac{g^{V\,2}_{\Delta\Delta\rho}}{4\pi}=4.69$	1400
		$\frac{g^T_{\Delta\Delta\rho}}{g^V_{\Delta\Delta\rho}}=6.1$	
$\pi\pi\rho$	ρ exchange	$\frac{g^2_{\pi\pi\rho}}{4\pi}=2.90$	1400
$NN\sigma$	$N-$, σ exchange	$\frac{g^2_{NN\sigma}}{4\pi}=13$	2000
$\sigma\sigma\sigma$	σ exchange	$\frac{g_{NN\sigma}g_{\sigma\sigma\sigma}}{4\pi}=2.85$	2000
$NN\eta$	N exchange	$\frac{f^2_{NN\eta}}{4\pi}=0.00934$	2500
NNa_0, $\pi\eta a_0$	a_0 exchange	$\frac{g_{NNa_0}g_{\pi\eta a_0}}{4\pi}=8.0$	2500
$NN^{*\,S11}_{1535}\pi$	N^* pole, $m^0_{N^*}=1660$	$\frac{g^2_{NN^*\pi}}{4\pi}=0.001$	3000
$NN^{*\,S11}_{1535}\eta$	N^* pole, $m^0_{N^*}=1660$	$\frac{g^2_{NN^*\eta}}{4\pi}=0.30$	3000
$NN^{*\,S11}_{1650}\pi$	N^* pole, $m^0_{N^*}=1770$	$\frac{g^2_{NN^*\pi}}{4\pi}=0.16$	3000

tion channel. The parameters for this coupled-channels model (model D) are given in Table V. (The coupling of the ηN channel turns out to be of no importance for the $P11$ partial wave.) As one can see in Fig. 11, we obtain with this model a good description of both the phase shift and the inelasticity. In the region of the Roper resonance, the Karlsruhe-Helsinki analysis [27] and the more recent VPI analysis [28] differ significantly from one another. Our model achieves a good agreement with the Karlsruhe-Helsinki analysis. Especially conspicuous here is the plateau in the phase shift beginning at an energy of about 1.55 GeV which both the data and our model reach.

The quantitative description of the inelasticity requires a contribution from the diagonal σN interaction. In our model the effective coupling strength for the σ exchange in this channel is taken as a freely adjustable parameter. In combination with the potential for nucleon exchange, this coupling strength provides a measure of the strength of the diagonal interaction in the σN channel. By taking into account the self-energy in the propagation of the σN intermediate state we also obtain a qualitatively good description of the inelasticity in the threshold region.

In our model, the σN reaction channel plays a larger role than the $\pi\Delta$ channel in the description of the Roper resonance. This is in apparent disagreement with the results of the Particle Data Group [40], which estimates the contribution of the $\pi\Delta$ channel to the width of the Roper resonance as 20–30 %, while that of the σN only as 5–10 %. Their results are based, however, on a resonance model analysis of the πN scattering amplitude. In such an analysis the scattering data is inherently parametrized by ''genuine'' resonances. The strong nonpole interaction which we obtain in our model is therefore not considered. This emphasizes the model dependence of the results of the Particle Data Group [40], and of our model as well, in the description of the Roper resonance.

IV. THE FULL COUPLED-CHANNEL MODEL OF THE πN INTERACTION

In comparison with our basic (elastic) model, we have, with the construction of the coupled $\pi N/\eta N/\pi\Delta/\sigma N$ channels model (model D) for the $P11$ partial wave, been able to double the energy range for which the model describes the scattering data. We here show what picture this full model yields for the other partial waves. The complete results for the isospin $\frac{1}{2}$ channel are shown in Fig. 12 and those for the isospin $\frac{3}{2}$ channel in Fig. 13.

Since for the coupling of the ηN channel we have used almost the same parameter as in model B3 of Sec. II, we obtain equivalent results for the $S11$ partial wave.

In the $P13$ partial wave our model gives somewhat too much repulsion. This phase, however, in the energy range under consideration, accounts for very little cross section, so that the absolute difference of the model from the data is significantly smaller than the relative difference. Moreover, one must consider the fact that there is an experimentally well-established resonance in this partial wave [$N^*_{P13}(1720)$] which predominantly couples to the ρN channel [40]. It is therefore almost certain that the inclusion of the coupling to the ρN channel, which we have so far neglected in our model, would give attraction in $P13$ partial wave. In this sense the divergence of the results of our model from the data can be understood. Work on coupling the ρN channel is currently in progress.

In the $D13$ partial wave our model, in its current form, yields only a background for the resonance $N^*_{D13}(1520)$. Here we could achieve a good representation of the data by the additional contribution of a $N^*_{D13}(1520)$ pole diagram.

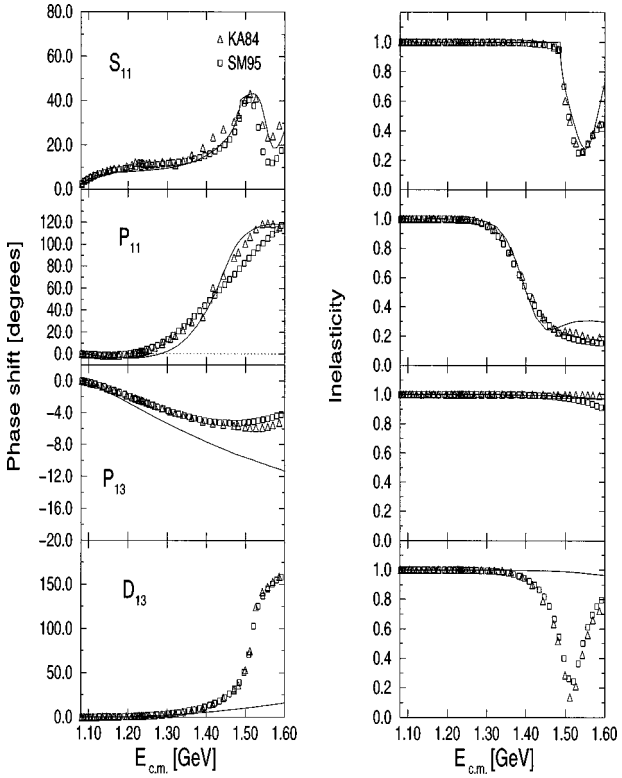

FIG. 12. Results for the full coupled-channels model (model D) for the πN phase shifts and inelasticities in the isospin channel $I=\frac{1}{2}$ compared with the empirical data from the Karlsruhe-Helsinki analysis KA84 [27] (triangles) and the VPI analysis SM95 [28] (squares).

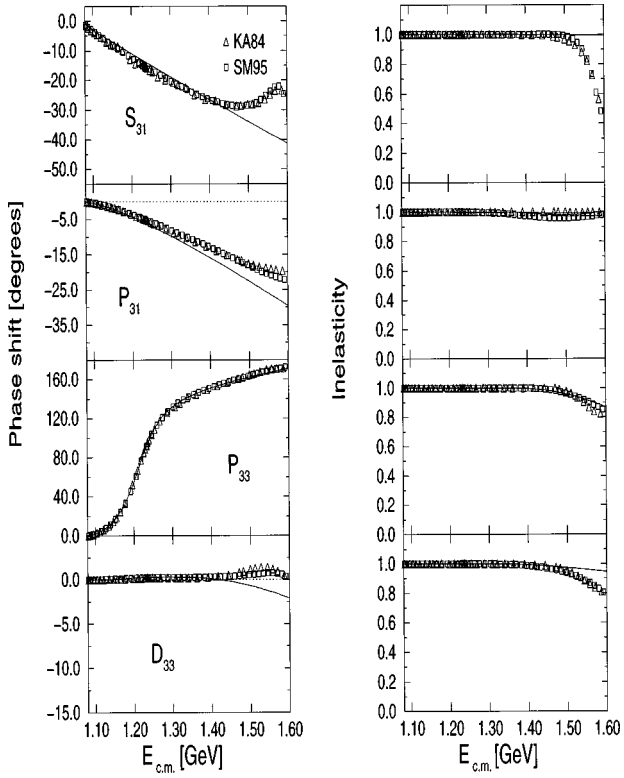

FIG. 13. Results for the full coupled-channels model (model D) for the πN phase shifts and inelasticities in the isospin channel $I=\frac{3}{2}$ compared with the empirical data from the Karlsruhe-Helsinki analysis KA84 [27] (triangles) and the VPI analysis SM95 [28] (squares).

However, in the context of our model, this would only be a parametrization of the data and will not be pursued further. Were we to do this, however, then the influence of the ρN should also be investigated. (Aaron *et al.* [42] have developed a coupled $\pi N/\rho N$ channel model which produces a dynamical resonance in the $D13$ wave. However, it reproduces the $D13$ data only qualitatively, with the resonance lying at too high an energy.)

At this point it should be remembered that in the present model only the πN and $\pi\Delta$ reaction channels contribute to the isospin $\frac{3}{2}$ partial waves. As one can observe in Fig. 13, the resonance $\Delta^*_{S31}(1620)$ cannot be produced dynamically in our model through the $\pi\Delta$ channel. The coupling of the $\pi\Delta$ channel to the πN system is weak in this partial wave, as a $J=\frac{1}{2}$ $\pi\Delta$ system cannot be in an S state. The coupling to the πN S wave is therefore only possible through the relatively weak tensor transition. While the model yields a nearly perfect fit to the $P33$ partial wave data, there are small differences at higher energies in the $P31$ and $D33$ partial waves.

It is clear that a precise fit to the data, already in this relatively low-energy range, is complicated by the growing influence of numerous nucleon and Δ resonances. Nevertheless, on the whole, our model achieves a fairly good description of the πN scattering data in the domain below the onset of these known resonances.

V. SUMMARY AND OUTLOOK

In this and previous work [3,4] we have developed a meson exchange model for the pion-nucleon interaction which gives a fairly good description of the empirical πN scattering data in the elastic, as well as in the inelastic energy region, up to an energy of $E_{\text{c.m.}}\approx 1.4$ GeV, and even up to ≈ 1.6 GeV in partial waves not yet influenced by the onset of known resonances or opening inelastic channels.

The origin of our investigation was a dynamical model for the correlated 2π exchange in the πN interaction. In combination with pole and exchange contributions of the nucleon and Δ, we constructed a model for the elastic pion-nucleon interaction. Already in our single-channel model we obtained a quantitative description of the elastic scattering. The inclusion of different contributions to the interaction in the $P33$ partial wave in the framework of this microscopic model indicated the importance of the nonpole parts of the interaction for the understanding of the Δ isobar.

The single-channel model of I and II forms a suitable starting point for many applications in intermediate-energy physics in which the πN interaction at low energy plays a role. Examples of this would be pion production in NN scattering [43] and pion photoproduction [44]. In both processes the interaction of the πN system in the final state is of great importance.

To extend the model in order to apply it to higher energies, we have been led to include the coupling of more reaction channels, and to use a coupled-channels approach to take inelasticity into account. The ultimate goal of our investigations has been a better understanding of the observed spectrum of nucleon and Δ resonances. Towards this goal, we have attempted to see whether there are clear signs that

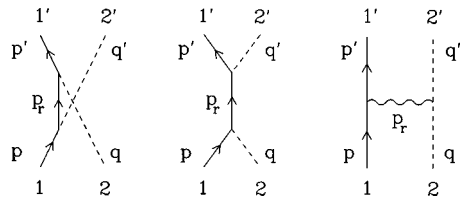

FIG. 14. Baryon exchange, pole, and meson exchange diagram for defining the notation.

these resonances contain genuine three-quark cores, or whether they can be understood solely on the basis of interactions of nucleons and their meson clouds. In this regard we find that the $N^*_{S11}(1535)$ cannot be well described without the pole-type contribution. We see this as evidence for an underlying three-quark structure of the resonance. The situation for the Roper resonance looks quite different, however. One of the major conclusions of this work is that it is possible, in the framework of a coupled $\pi N/\pi\Delta/\sigma N$ system, to explain the Roper resonance as a dynamical effect. The coupling of the σN channel is of particular importance to this understanding.

The full coupled $\pi N/\eta N/\pi\Delta/\sigma N$ channels model that we have developed in this work forms a suitable basis for further investigations of the baryon spectrum. As a next step in this development, the coupling of the ρN channel would logically come into consideration. Even in the limited energy range we have treated, this reaction channel could already play a noticeable role. Were one to treat the ρ meson as a gauge boson of a local chiral transformation [41], one would then have, among other effects, a three-ρ vertex, which would then result in a contribution through ρ exchange to a diagonal ρN interaction. It is quite possible that this potential would play a similar role as our phenomenological σ exchange in the σN channel.

In the framework of such an expanded model, the question of the nature of the resonances $N^*_{D13}(1520)$ and $\Delta_{S31}(1620)$ can be addressed. In the model considered so far, we have not found any signs of a dynamical origin for either resonance, but the question still remains open in the context of a more complete model.

In the work we have presented here, we have consciously limited the investigation of πN scattering to hadronic interactions. As further steps, building on the knowledge gained here, one should next strive for a consistent description of photoproduction and electroproduction of pions and η mesons, as well as of electromagnetic excitation of nucleon resonances.

ACKNOWLEDGMENT

We are grateful to our late colleague and friend, Karl Holinde, for his essential contributions to this work.

APPENDIX: THE POTENTIALS

In this appendix we give the expressions for the potentials from the different contributions to our interaction model in the ηN, $\pi\Delta$, and σN reaction channels. The notation for the different particles and their momenta is given in Fig. 14. In the expressions we use, for compactness, $E_r=\omega_r=\sqrt{m_r^2+\vec{p}_r^{\,2}}$; for the baryon resonance pole graphs $p_r^0=\sqrt{s}$ and for the baryon exchange graphs $p_r^0=\epsilon_1-\epsilon_{2'}$, with $\epsilon_1\equiv(s+m_1^2-m_2^2)/2\sqrt{s}$ and $\epsilon_{2'}\equiv(s-m_{1'}^2+m_{2'}^2)/2\sqrt{s}$. E_p, $E_{p'}$, ω_q, and $\omega_{q'}$ indicating on-mass-shell energies of baryons 1 and $1'$ and, respectively, those of mesons 2 and $2'$:

$$E_{p^{(\prime)}}=\sqrt{m_{1^{(\prime)}}^2+\vec{p}^{\,(\prime)\,2}};\quad \omega_{q^{(\prime)}}=\sqrt{m_{2^{(\prime)}}^2+\vec{q}^{\,(\prime)\,2}}. \tag{A1}$$

Since we work in time-ordered perturbation theory, all the potentials contain the normalization factor

$$\kappa=\frac{1}{(2\pi)^3}\sqrt{\frac{m_1}{E_p}\frac{m_{1'}}{E_{p'}}}\sqrt{\frac{1}{2\omega_q 2\omega_{q'}}}. \tag{A2}$$

In addition, all the potentials must be multiplied by the isospin factor $IF(I)$. These factors are given in Table VI at the end of this appendix.

TABLE VI. Isospin factors for the coupled channel system $\pi N/\eta N/\sigma N/\pi\Delta$.

reaction channel	Process	$IF(\frac{1}{2})$	$IF(\frac{3}{2})$
$\pi N\to\pi N$	N pole graph	3	0
	N exchange	-1	2
	Δ pole graph	0	1
	Δ exchange	$\frac{4}{3}$	$\frac{1}{3}$
	N^*_{S11} pole graph	3	0
$\pi N\to\eta N$	N^*_{S11} pole graph	$\sqrt{3}$	0
	N exchange	$\sqrt{3}$	0
	a_0 exchange	$\sqrt{3}$	0
$\eta N\to\eta N$	N^*_{S11} pole graph	1	0
	N exchange	1	0
	f_0 exchange	1	0
$\pi N\to\sigma N$	N exchange	$\sqrt{3}$	0
$\sigma N\to\sigma N$	N exchange	1	0
	σ exchange	1	0
$\pi N\to\pi\Delta$	N exchange	$-\sqrt{\frac{8}{3}}$	$\sqrt{\frac{5}{3}}$
	Δ exchange	$-\frac{5}{3}\sqrt{\frac{2}{3}}$	$-\frac{10}{3\sqrt{15}}$
	ρ exchange	$\sqrt{\frac{2}{3}}$	$\sqrt{\frac{5}{3}}$
$\pi\Delta\to\pi\Delta$	N exchange	$\frac{1}{3}$	$-\frac{2}{3}$
	Δ exchange	$-\frac{10}{9}$	$\frac{11}{9}$
	ρ exchange	$\frac{5}{3}$	$\frac{2}{3}$

1. The coupling of the ηN channel

For the contributions to the transition interaction $\pi N \to \eta N$ and to the direct (diagonal) ηN interaction from Fig. 1 one finds from the interaction Lagrangian (Eq. 2.1), the following expressions.

(a) nucleon exchange $\pi N \to \eta N$ and, respectively, $\eta N \to \eta N$:

$$\langle \vec{p}\,'\lambda'|V_N^{\rm ex}(Z)|\vec{p}\,\lambda\rangle = \kappa \frac{f_{NN\pi(\eta)} f_{NN\eta}}{m_\pi^2} q_\mu q'_\nu \overline{u}(\vec{p}\,',\lambda')\gamma^5\gamma^\mu \frac{1}{2E_r}\left(\frac{\gamma^0 E_r - \vec{\gamma}\vec{p}_r + m_N}{Z - E_r - \omega_q - \omega_{q'}} + \frac{-\gamma^0 E_r - \vec{\gamma}\vec{p}_r + m_N}{Z - E_r - E_p - E_{p'}}\right) \times \gamma^5\gamma^\nu u(\vec{p}\,,\lambda)\; IF(I). \tag{A3}$$

(b) a_0 exchange $\pi N \to \eta N$:

$$\langle \vec{p}\,'\lambda'|V_{a_0}^{\rm ex}(Z)|\vec{p}\,\lambda\rangle = \kappa\; g_{NNa_0} g_{\pi\eta a_0} m_\pi\; \overline{u}(\vec{p}\,',\lambda') u(\vec{p}\,,\lambda)\; IF(I) \frac{1}{2\omega_r}\left(\frac{1}{Z - \omega_r - E_{p'} - \omega_q} + \frac{1}{Z - \omega_r - E_p - \omega_{q'}}\right). \tag{A4}$$

(c) f_0 exchange $\eta N \to \eta N$:

$$\langle \vec{p}\,'\lambda'|V_{f_0}^{\rm ex}(Z)|\vec{p}\,\lambda\rangle = \kappa\; 2\, g_{NNf_0} g_{\eta\eta f_0} m_\pi\; \overline{u}(\vec{p}\,',\lambda') u(\vec{p}\,,\lambda)\; IF(I) \frac{1}{2\omega_r}\left(\frac{1}{Z - \omega_r - E_{p'} - \omega_q} + \frac{1}{Z - \omega_r - E_p - \omega_{q'}}\right). \tag{A5}$$

(d) N^* pole diagram $\pi N \to \eta N$ and, correspondingly, $\eta N \to \eta N$:

$$\langle \vec{p}\,'\lambda'|V_{N^*_{S11}}(Z)|\vec{p}\,\lambda\rangle = \kappa\; g_{N^*N\pi(\eta)} g_{N^*N\eta} \overline{u}(\vec{p}\,',\lambda') \frac{\gamma_0 m_{N^*} + m_{N^*}}{2m_{N^*}(Z - m_{N^*})} u(\vec{p},\lambda)\; IF(I). \tag{A6}$$

2. The reaction channel $\pi\Delta$

a. The transition interaction $\pi N \to \pi\Delta$

(a) nucleon exchange:

$$\langle \vec{p}\,'\lambda'|V_N^{\rm ex}(Z)|\vec{p}\,\lambda\rangle = \kappa \frac{f_{NN\pi} f_{N\Delta\pi}}{m_\pi^2} q_\mu q'_\nu \overline{u}^\mu(\vec{p}\,',\lambda') \frac{1}{2E_r}\left(\frac{\gamma^0 E_r - \vec{\gamma}\vec{p}_r + m_N}{Z - E_r - \omega_q - \omega_{q'}} + \frac{-\gamma^0 E_r - \vec{\gamma}\vec{p}_r + m_N}{Z - E_r - E_p - E_{p'}}\right) \gamma^5\gamma^\nu u(\vec{p}\,,\lambda)\; IF(I). \tag{A7}$$

(b) Δ exchange:

$$\langle \vec{p}\,'\lambda'|V_\Delta^{\rm ex}(Z)|\vec{p}\,\lambda\rangle = \kappa \frac{f_{N\Delta\pi} f_{\Delta\Delta\pi}}{m_\pi^2} q_\tau q'_\nu \overline{u}_\mu(\vec{p}\,',\lambda')\gamma^5\gamma^\tau(\not{p}_r + m_\Delta)\left\{-g^{\mu\nu} + \frac{1}{3}\gamma^\mu\gamma^\nu + \frac{2}{3m_\Delta^2} p_r^\mu p_r^\nu - \frac{1}{3m_\Delta}(p_r^\mu\gamma^\nu - p_r^\nu\gamma^\mu)\right\} \times u(\vec{p}\,,\lambda) \frac{1}{2E_r}\left(\frac{1}{Z - E_r - \omega_q - \omega_{q'}} + \frac{1}{Z - E_r - E_p - E_{p'}}\right)\; IF(I). \tag{A8}$$

(c) ρ exchange:

$$\langle \vec{p}\,'\lambda'|V_\rho^{\rm ex}(Z)|\vec{p}\,\lambda\rangle = \kappa \frac{f_{N\Delta\rho} g_{\pi\pi\rho}}{m_\rho}\{\overline{u}_\nu(\vec{p}\,',\lambda')\gamma^5\gamma_\mu p_r^\mu u(\vec{p}\,,\lambda)\; (q+q')^\nu - \overline{u}_\nu(\vec{p}\,',\lambda')\gamma^5\gamma_\mu(q+q')^\mu u(\vec{p}\,,\lambda)\; p_r^\nu\} \times \frac{1}{2\omega_r}\left(\frac{1}{Z - \omega_r - E_{p'} - \omega_q} + \frac{1}{Z - \omega_r - E_p - \omega_{q'}}\right)\; IF(I). \tag{A9}$$

b. The diagonal $\pi\Delta$ interaction

(a) nucleon exchange:

$$\langle \vec{p}\,'\lambda'|V_N^{\rm ex}(Z)|\vec{p}\,\lambda\rangle=\kappa\frac{f_{N\Delta\pi}^2}{m_\pi^2}q_\mu q'_\nu\overline{u^\mu}(\vec{p}\,',\lambda')\frac{1}{2E_r}\left(\frac{\gamma^0E_r-\vec{\gamma}\vec{p}_r+m_N}{Z-E_r-\omega_q-\omega_{q'}}+\frac{-\gamma^0E_r-\vec{\gamma}\vec{p}_r+m_N}{Z-E_r-E_p-E_{p'}}\right)u^\nu(\vec{p}\,,\lambda)\ IF(I). \quad \text{(A10)}$$

(b) Δ exchange:

$$\langle \vec{p}\,'\lambda'|V_\Delta^{\rm ex}(Z)|\vec{p}\,\lambda\rangle=\kappa\frac{f_{\Delta\Delta\pi}^2}{m_\pi^2}q_\tau q'_\delta\overline{u}_\mu(\vec{p}\,',\lambda')\gamma^5\gamma^\tau(\not{p}_r+m_\Delta)\left\{-g^{\mu\nu}+\frac{1}{3}\gamma^\mu\gamma^\nu+\frac{2}{3m_\Delta^2}p_r^\mu p_r^\nu-\frac{1}{3m_\Delta}(p_r^\mu\gamma^\nu-p_r^\nu\gamma^\mu)\right\}$$
$$\times\gamma^5\gamma^\delta u_\nu(\vec{p}\,,\lambda)\frac{1}{2E_r}\left(\frac{1}{Z-E_r-\omega_q-\omega_{q'}}+\frac{1}{Z-E_r-E_p-E_{p'}}\right)\ IF(I). \quad \text{(A11)}$$

(c) ρ exchange:

$$\langle \vec{p}\,'\lambda'|V_\rho^{\rm ex}(Z)|\vec{p}\,\lambda\rangle=\kappa\ g_{\pi\pi\rho}\ \overline{u}_\nu(\vec{p}\,',\lambda')\left\{(g_{\Delta\Delta\rho}^T+g_{\Delta\Delta\rho}^V)\gamma^\mu-\frac{g_{\Delta\Delta\rho}^T}{2m_\Delta}(p+p')^\mu\right\}u^\nu(\vec{p}\,,\lambda)\ (q+q')_\mu\frac{1}{2\omega_r}$$
$$\times\left(\frac{1}{Z-\omega_r-E_{p'}-\omega_q}+\frac{1}{Z-\omega_r-E_p-\omega_{q'}}\right)\ IF(I). \quad \text{(A12)}$$

In the calculation of ρ-exchange potentials of the form of Eq. (A12), in analogy to the calculation of the ρ exchange in the Bonn potential for the NN interaction [25], the Gordon decomposition (here at the $\Delta\Delta\rho$ vertex) has been used.

3. The reaction channel σN

(a) nucleon exchange $\pi N\to\sigma N$:

$$\langle \vec{p}\,'\lambda'|V_N^{\rm ex}(Z)|\vec{p}\,\lambda\rangle=-i\ \kappa\ \frac{f_{NN\pi}g_{NN\sigma}}{m_\pi}q_\mu\overline{u}(\vec{p}\,',\lambda')\ \gamma^5\gamma^\mu\frac{1}{2E_r}\left(\frac{\gamma^0E_r-\vec{\gamma}\vec{p}_r+m_N}{Z-E_r-\omega_q-\omega_{q'}}+\frac{-\gamma^0E_r-\vec{\gamma}\vec{p}_r+m_N}{Z-E_r-E_p-E_{p'}}\right)u(\vec{p}\,,\lambda)\ IF(I). \quad \text{(A13)}$$

(b) nucleon exchange $\sigma N\to\sigma N$:

$$\langle \vec{p}\,'\lambda'|V_N^{\rm ex}(Z)|\vec{p}\,\lambda\rangle=\kappa\ g_{NN\sigma}^2\overline{u}(\vec{p}\,',\lambda')\frac{1}{2E_r}\left(\frac{\gamma^0E_r-\vec{\gamma}\vec{p}_r+m_N}{Z-E_r-\omega_q-\omega_{q'}}+\frac{-\gamma^0E_r-\vec{\gamma}\vec{p}_r+m_N}{Z-E_r-E_p-E_{p'}}\right)u(\vec{p}\,,\lambda)\ IF(I). \quad \text{(A14)}$$

(c) σ exchange $\sigma N\to\sigma N$:

$$\langle \vec{p}\,'\lambda'|V_\sigma^{\rm ex}(Z)|\vec{p}\,\lambda\rangle=\kappa\ 6\ g_{NN\sigma}g_{\sigma\sigma\sigma}m_\sigma\ \overline{u}(\vec{p}\,',\lambda')u(\vec{p}\,,\lambda)\ IF(I)\frac{1}{2\omega_r}\left(\frac{1}{Z-\omega_r-E_{p'}-\omega_q}+\frac{1}{Z-\omega_r-E_p-\omega_{q'}}\right). \quad \text{(A15)}$$

4. Isospin factors

We show in Table VI the isospin factor $IF(I)$ to be used in the expressions for the potentials given above.

[1] D. Lohse, J. W. Durso, K. Holinde, and J. Speth, Nucl. Phys. **A516**, 513 (1990).

[2] M. Hoffmann, J. W. Durso, K. Holinde, B. C. Pearce, and J. Speth, Nucl. Phys. **A593**, 341 (1995).

[3] C. Schütz, J. W. Durso, K. Holinde, and J. Speth, Phys. Rev. C **49**, 2671 (1994).

[4] C. Schütz, J. W. Durso, K. Holinde, B. C. Pearce, and J. Speth, Phys. Rev. C **51**, 1374 (1995).

[5] H.-C. Kim, J. W. Durso, and K. Holinde, Phys. Rev. C **49**, 2355 (1994); A. Reuber, K. Holinde, H.-C. Kim, and J. Speth, Nucl. Phys. **A608**, 243 (1996).

[6] T. Cheng and R. Dashen, Phys. Rev. Lett. **26**, 594 (1971).

[7] R. A. Arndt, R. L. Workman, Z. Li, and L. D. Roper, Phys. Rev. C **42**, 1853 (1990).

[8] H. N. K. Sarma *et al.*, Nucl. Phys. **B161**, 1 (1979).

[9] B. M. K. Nefkens, in *Proceedings of the International Confer-*

ence on ''Mesons and Nuclei at Intermediate Energies,'' Dubna, Russia, 1994 (World Scientific, Singapore, 1995).
[10] M. Clajus and B. M. K. Nefkens, πN Newsletter **7**, 76 (1992).
[11] B. Krusche *et al.*, Phys. Rev. Lett. **74**, 3736 (1995).
[12] B. Schoch, Prog. Part. Nucl. Phys. **35**, 43 (1995).
[13] H. S. Plendl and H. Machner, in Ref. [9].
[14] H. Calén *et al.*, Phys. Lett. B **366**, 39 (1996).
[15] M. Batinić, I. Dadić, I. Šlaus, A. Švarc, B. M. K. Nefkens, and T.-S. H. Lee, nucl-th/9703023; M. Batinić, I. Šlaus, and A. Švarc, Phys. Rev. C **52**, 2188 (1995); M. Batinić, I. Šlaus, A. Švarc, and B. M. K. Nefkens, *ibid.* **51**, 2310 (1995).
[16] R. S. Bhalerao and L. C. Liu, Phys. Rev. Lett. **54**, 865 (1985).
[17] Ch. Sauermann, B. L. Friman, and W. Nörenberg, Phys. Lett. B **341**, 261 (1995).
[18] G. Höhler, in *Physics with GeV-Particle Beams*, edited by H. Machner and K. Sistemich (World Scientific, Singapore, 1995), p. 198; G. Höhler and A. Schulte, πN Newsletter **7**, 94 (1992).
[19] N. Isgur and G. Karl, Phys. Rev. D **18**, 4187 (1978).
[20] N. Isgur and G. Karl, Phys. Rev. D **19**, 2653 (1979).
[21] L. Ya Glozman and D. O. Riska, Phys. Rep. **268**, 263 (1996).
[22] G. Janssen, K. Holinde, B. C. Pearce, and J. Speth, Phys. Rev. D **52**, 2690 (1995).
[23] J. J. de Swart, Rev. Mod. Phys. **35**, 916 (1963).
[24] A. Pais, Rev. Mod. Phys. **38**, 215 (1966).
[25] R. Machleidt, K. Holinde, and Ch. Elster, Phys. Rep. **149**, 1 (1987).
[26] N. Kaiser, T. Waas, and W. Weise, Nucl. Phys. **A612**, 297 (1997); N. Kaiser, P. B. Siegel, and W. Weise, Phys. Lett. B **362**, 23 (1995).
[27] G. Höhler (private communication).
[28] R. A. Arndt, I. I. Strakovsky, R. L. Workman, and M. M. Pavan, Phys. Rev. C **52**, 2120 (1995).
[29] W. Deinet *et al.*, Nucl. Phys. **B11**, 495 (1969).
[30] F. Bulos *et al.*, Phys. Rev. **187**, 1827 (1969).
[31] W. B. Richards *et al.*, Phys. Rev. D **1**, 10 (1970).
[32] H. P. Morsch *et al.*, Phys. Rev. Lett. **69**, 1336 (1992).
[33] G. E. Brown, J. W. Durso, and M. B. Johnson, Nucl. Phys. **A397**, 447 (1983).
[34] B. C. Pearce and I. R. Afnan, Phys. Rev. C **40**, 220 (1989).
[35] G. Brown and W. Weise, Phys. Rep. **22**, 279 (1975).
[36] J. W. Durso, A. D. Jackson, and B. J. Verwest, Nucl. Phys. **A345**, 471 (1980).
[37] R. Koch and E. Pietarinen, Nucl. Phys. **A336**, 331 (1980).
[38] C. D. Froggatt and J. L. Petersen, Nucl. Phys. **B129**, 89 (1977).
[39] B. C. Pearce and I. R. Afnan, Phys. Rev. C **34**, 991 (1986).
[40] Particle Data Group, L. Montanet *et al.*, Phys. Rev. D **50**, 1173 (1994).
[41] M. Bando, T. Kugo, and K. Yamawaki, Phys. Rep. **164**, 217 (1988).
[42] R. Aaron, D. C. Teplitz, R. D. Amado, and J. E. Young, Phys. Rev. **187**, 2047 (1969).
[43] C. Hanhart, J. Haidenbauer, A. Reuber, C. Schütz, and J. Speth, Phys. Lett. B **358**, 21 (1995); J. Haidenbauer, C. Hanhart, and J. Speth, Acta Phys. Pol. B **27**, 2893 (1996).
[44] K. Nakayama, C. Schütz, S. Krewald, J. Speth, and W. Pfeil, in *Proceedings of the Fourth CEBAF/INT Workshop on N* Physics*, edited by T.-S. H. Lee and W. Roberts (World Scientific, Singapore, 1997), p. 156.